Mean-Square Optical Anisotropy of Isotactic Oligo- and Poly(methyl methacrylate)s in Dilute Solution

Yoshio Takaeda, Takenao Yoshizaki, and Hiromi Yamakawa*

Department of Polymer Chemistry, Kyoto University, Kyoto 606-01, Japan

Received November 17, 1994; Revised Manuscript Received March 13, 1995[⊗]

ABSTRACT: The mean-square optical anisotropy $\langle\Gamma^2\rangle$ was determined from anisotropic light-scattering measurements for 10 samples of isotactic oligo- and poly(methyl methacrylate)s (i-PMMA), each with the fraction of racemic diads $f_r \simeq 0.01$, in the range of weight-average molecular weight from 3.58×10^2 (trimer) to 1.07×10^4, and also for methyl isobutyrate (the monomer of PMMA), in acetonitrile at 28.0 °C (Θ). A comparison is made of the present data with the helical wormlike (HW) chain theory with the values of the model parameters previously determined from the mean-square radius of gyration $\langle S^2\rangle$ and with the local polarizability tensor properly assigned to the repeat unit of the chain in the same manner as in the previous study of atactic (a-) PMMA, i.e., evaluated with the same bond polarizabilities. It is shown that the HW theoretical values may reproduce quantitatively the experimental results in the range of weight-average degree of polymerization $x_w \geq 6$. The disagreement between theory and experiment for $x_w \leq 5$ may probably be due to effects of chain ends. A comparison is also made of the present results with the previous ones for a-PMMA, leading to the conclusion that the HW theory may explain the f_r dependence of $\langle\Gamma^2\rangle$ as well as of $\langle S^2\rangle$, the scattering function, and steady-state transport coefficients.

Introduction

In previous papers,[1-3] we made an experimental study of the mean-square radius of gyration[1] $\langle S^2\rangle$, scattering function[2] $P(k)$, and steady-state transport coefficients[3] for isotactic poly(methyl methacrylate) (i-PMMA) with the fraction of racemic diads $f_r \simeq 0.01$ in the unperturbed state, i.e., in acetonitrile (CH_3CN) at 28.0 °C (Θ). The data obtained for them over a wide range of weight-average molecular weight M_w, including the oligomer region with very low M_w, were analyzed on the basis of the helical wormlike (HW) chain,[4,5] and its model parameters for i-PMMA were determined rather unambiguously. From a comparison of the values of the model parameters thus obtained with those previously[6-8] determined for atactic (a-) PMMA with $f_r = 0.79$, it has then been shown that the difference in f_r causes drastic changes in the stiffness and local conformation of the PMMA chain or its helical nature.[1,9] It is known that the dependence on M_w of the mean-square optical anisotropy $\langle\Gamma^2\rangle$ also provides useful information about local chain conformations,[10] and in fact, we had already made its experimental study for atactic oligo- and polystyrenes (a-PS)[11] and a-PMMA.[12] Thus, in the present paper, we carry out measurements of $\langle\Gamma^2\rangle$ for i-PMMA in CH_3CN at 28.0 °C and examine its dependence on f_r by comparing the results with those previously obtained for a-PMMA.[12]

In the previous study of a-PMMA,[12] from a comparison between the HW theoretical and observed values of the ratio of $\langle\Gamma^2\rangle$ to the weight-average degree of polymerization x_w, it has been found that the theoretical value 14.3 Å^6 of the ratio $(\langle\Gamma^2\rangle/x_w)_\infty$ in the limit $x_w \to \infty$ calculated with the local polarizability tensor $\boldsymbol{\alpha}_0$ properly assigned to the repeat unit of the a-PMMA chain is appreciably larger than the observed value 7.8 Å^6. We have regarded this disagreement between the theoretical and observed values as arising from the fact that the effective (true) polarizability of the ester group in the PMMA chain, whose value is necessary for a correct evaluation of $\boldsymbol{\alpha}_0$, is somewhat smaller than that of methyl acetate used for the actual evaluation of $\boldsymbol{\alpha}_0$. It has then been shown that the disagreement can be removed simply by replacing $\boldsymbol{\alpha}_0$ by $0.73\boldsymbol{\alpha}_0$; i.e., with this minor modification, the dependence of $\langle\Gamma^2\rangle/x_w$ on x_w may be well explained by the HW theory. Although this modification is only empirical and cannot be justified theoretically, the values of $\boldsymbol{\alpha}_0$ themselves are not important as far as major attention is given to the dependence of $\langle\Gamma^2\rangle$ on f_r. In other words, the present important problem is to examine whether the difference in the behavior of $\langle\Gamma^2\rangle$ between the i- and a-PMMAs may be explained by the HW theory with the use of their $\boldsymbol{\alpha}_0$'s (or $0.73\boldsymbol{\alpha}_0$'s) evaluated with the same bond polarizabilities.

As in the case of a-PMMA, the optical anisotropy of i-PMMA is small (compared to a-PS), while that of CH_3CN used as a Θ solvent, which was used as a Θ solvent also for a-PMMA,[12] is rather large (compared to cyclohexane, i.e., a Θ solvent for a-PS). Thus, for an accurate determination of the excess depolarized scattering intensity for i-PMMA in CH_3CN, we measure the spectra of the light scattered from the solution and solvent by the use of a Fabry–Perot (FP) interferometer, as done in the previous study.[12]

There may be an objection to the determination of $\langle\Gamma^2\rangle$ in the optically anisotropic solvent CH_3CN even if the FP spectrometer is used. This is because it is in principle very difficult to separate the excess (intrinsic) depolarized component due to solute molecules in such a solvent. However, it has been shown in the previous study[12] of $\langle\Gamma^2\rangle$ of a-PMMA that the value 4.1_6 Å^6 of $\langle\Gamma^2\rangle$ of methyl isobutyrate (MIB), the monomer of PMMA, determined in CH_3CN at 44.0 °C is in fairly good agreement with the value 3.7_2 Å^6 determined in the optically isotropic solvent carbon tetrachloride (CCl_4) at 25.0 °C. Furthermore, it has also been shown in our recent dynamic depolarized light-scattering study of a-PMMA[13] that both the spectra of the excess depolarized components of light scattered from the solutions of MIB in the above two solvents may be well fitted by single Lorentzians and that the values of the reduced relaxation time as defined as the reciprocal of the half-width at half-maximum of these spectra multiplied by k_BT/η_0 with k_B the Boltzmann constant, T the absolute

[⊗] Abstract published in *Advance ACS Abstracts,* May 15, 1995.

0024-9297/95/2228-4167$09.00/0

Table 1. Values of M_w, x_w, and M_w/M_n for Isotactic Oligo- and Poly(methyl methacrylate)s

sample	M_w	x_w	M_w/M_n
MIB	1.02×10^2		
iOM3[a]	3.58×10^2	3	1.00
iOM4	4.58×10^2	4	1.00
iOM5	5.58×10^2	5	1.00
iOM6	6.58×10^2	6	1.00
iOM7	7.89×10^2	7.31	1.01
iOM10[b]	1.01×10^3	9.52	1.02
iOM18	1.79×10^3	17.3	1.10
iOM31	3.12×10^3	30.6	1.04
iOM71	7.07×10^3	70.1	1.05
iMM1	1.07×10^4	106	1.05

[a] M_w's of iOM3 through iOM7 had been determined from ^{1}H NMR and GPC.[1] [b] M_w's of iOM10 through iMM1 had been determined from LS in CH_3CN at 28.0 °C.[1,3]

temperature, and η_0 the solvent viscosity are 29.$_6$ and 28.$_6$ Å^3, respectively, and are in good agreement with each other. The above two facts indicate that the spectra in the two solvents may give essentially the same information about both static and dynamic properties and that possible effects of the optically anisotropic solvent are not very serious if any. In particular, such effects may be reduced in the present study where we are considering the dependence of $\langle\Gamma^2\rangle$ on molecular weight and stereochemical composition instead of its absolute value itself. Although it is better to determine $\langle\Gamma^2\rangle$ for all samples also in CCl_4, we avoid this since the exposure of solutions of PMMA in CCl_4 to a strong laser beam has proved to denature the precious samples and prevent their reuse, as mentioned in the previous paper.[12]

Experimental Section

Materials. All the i-PMMA samples used in this work are the same as those used in the previous studies[1-3] of $\langle S^2\rangle$, $P(k)$, the intrinsic viscosity $[\eta]$, and the translational diffusion coefficient D, i.e., the fractions separated by preparative gel permeation chromatography (GPC) or fractional precipitation from the original samples prepared by living anionic polymerization,[1] following the procedure of Ute et al.[14] They are sufficiently narrow in molecular weight distribution and have $f_r \simeq 0.01$ almost independent of M_w.[1] The values of M_w, x_w, and the ratio of M_w to the number-average molecular weight M_n previously determined[1,3] are summarized in Table 1.

MIB (Tokyo Kasei Kogyo Co.; 99.0% purity) was purified by distillation after dehydration by passing through a silica gel column, and the solvent CH_3CN was purified according to a standard procedure.

Anisotropic Light Scattering. The photometer used for all anisotropic light-scattering (LS) measurements is the same as that used in the previous study of a-PMMA,[12] i.e., a Brookhaven Instruments Model BI-200SM goniometer with a minor modification of its light source part and with a detector alignment newly assembled to incorporate an FP interferometer in it. It has been described in detail in the previous paper,[12] and therefore we here only give its short sketch (see Figure 1 of ref 12).

Vertically polarized light of wavelength 488 nm from a Spectra-Physics Model 2020 argon ion laser equipped with a Model 583 temperature-stabilized etalon for single-frequency-mode operation was used as a light source. It was made highly vertically (v) polarized by passing it through a Glan–Thompson (GT) prism with an extinction ratio smaller than 10^{-5}. The scattered light was measured at a scattering angle of 90°. Its horizontal (H) component, i.e., the depolarized (Hv) component, which was extracted from the total scattered light intensity by the use of the same GT prism as above, was analyzed with a Burleigh Instruments Model RC-110 FP interferometer equipped with a Model RC-670 pair of plane mirrors with a flatness of $\lambda/200$ and a reflectivity of 97.5%.

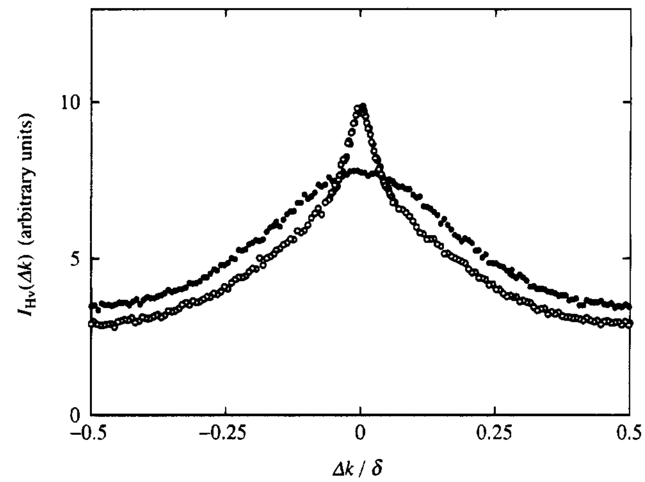

Figure 1. Plots of $I_{Hv}(\Delta k)$ against $\Delta k/\delta$: (○) i-PMMA sample iOM3 in CH_3CN at $c = 0.120$ g/cm^3 at 28.0 °C; (●) CH_3CN at 28.0 °C.

The intensity of the Hv component filtered through the FP interferometer was measured by an EMI 9893B/350 photomultiplier (PM) tube. As in the previous study,[12] we used a pinhole of diameter 100 μm as a spatial filter, which was placed between the interferometer and the PM tube. All the measurements were carried out in CH_3CN at 28.0 °C (Θ) by the single-passing operation of the interferometer, as in the previous study.[12]

The most concentrated solution of each sample was prepared gravimetrically and made homogeneous by continuous stirring for ca. 1 day at ca. 50 °C. These solutions and solvent were optically purified by filtration through a Teflon membrane of pore size 0.1 μm. The solutions of lower concentrations were obtained by successive dilution. As for the solutions of MIB, the solute was filtered and added to the purified solvent in a sample cell. The weight concentrations of the test solutions were converted to the solute mass concentrations c (in g/cm^3) by the use of the densities of the solutions.

Before and after each measurement on the solution or solvent, the spectrum of the Hv component scattered from pure benzene sealed in a Pyrex nuclear magnetic resonance tube of outer diameter 10 mm, which we used as a working standard (WS), was measured without a narrow band-pass filter in order to monitor any possible changes in the photometer system, as done in the previous static measurements.[12] Before every set of three measurements on pure benzene, on the solution or solvent, and again on benzene, the FP interferometer was tuned to obtain the highest finesse. The value of the finesse was 60–70 just after the tuning and usually decreased to 40–50 after the set of measurements, which took ca. 1 h. The free spectral range (FSR) was adjusted to be 5–50 cm^{-1}.

As an example, Figure 1 shows FP spectra of the depolarized component $I_{Hv}(\Delta k)$ of the scattered light intensity as a function of the wavenumber difference Δk between the incident and scattered light divided by the value δ of FSR for the solvent CH_3CN and for a solution of iOM3 in it at $c = 0.120$ g/cm^3 at 28.0 °C. All the values of I_{Hv} have been reduced by the total intensity of the Hv component for the WS determined from the measurements mentioned above.

As in the case of a-PMMA previously[12] studied, we may evaluate the excess Hv component $\Delta I_{Hv}(\Delta k)$ of the scattered light intensity from

$$\Delta I_{Hv}(\Delta k) = I_{Hv,soln}(\Delta k) - \phi I_{Hv,solv}(\Delta k) \quad (1)$$

with the values of $I_{Hv}(\Delta k)$ for the solution and solvent, where ϕ is the volume fraction of the solvent. Figure 2 shows spectra of $\Delta I_{Hv}(\Delta k)$ thus evaluated for the same solution of iOM3 in CH_3CN as in Figure 1 and for a solution of iOM71 in CH_3CN at $c = 0.125$ g/cm^3 at 28.0 °C.

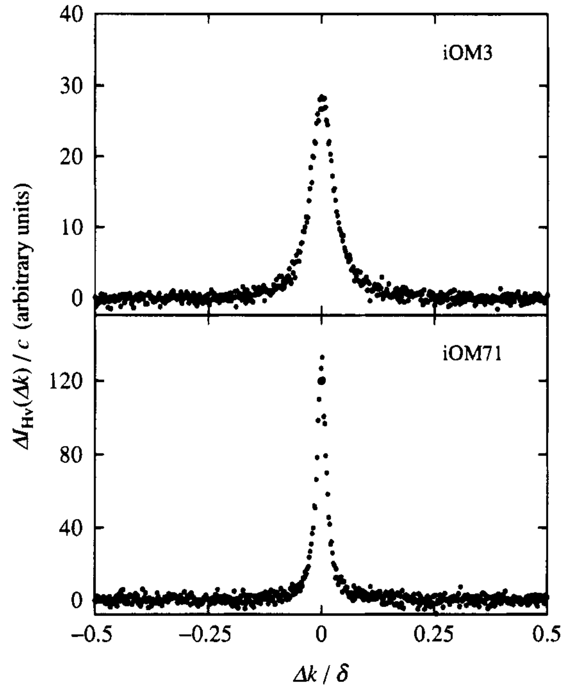

Figure 2. Plots of $\Delta I_{Hv}(\Delta k)$ against $\Delta k/\delta$ for i-PMMA samples iOM3 and iOM71 in CH_3CN at 28.0 °C.

As in the previous study,[12] the total intensity $\Delta I_{Hv,mol}$ of the intrinsic molecular part of the excess Hv component was evaluated by numerical integration of the observed quantity $\Delta I_{Hv}(\Delta k) - I_{base}$ over Δk in the range of one FSR, where I_{base} is the intensity of the flat base part of the FP spectrum.

Now the intrinsic molecular excess Hv component $\Delta R_{Hv,mol}$ of the reduced intensity may be calculated from

$$\Delta R_{Hv,mol} = \frac{\tilde{n}^2 \phi_A}{T_{max}} \Delta I_{Hv,mol} \quad (2)$$

with the value of $\Delta I_{Hv,mol}$ determined above, where $\tilde{n}$ is the refractive index of the solvent used, T_{max} is the maximum (or peak) transmittance of the narrow band-pass filter, and ϕ_A is the apparatus constant dependent on the photometer used. In eq 2, the $\tilde{n}^2$ correction of Hermans and Levinson[15] has been applied, and also a correction to $\Delta I_{Hv,mol}$ for the absorption by the narrow band-pass filter has been simply made by the factor $1/T_{max}$ since the width of the resultant spectrum of the excess scattering intensity (as shown in Figure 2) is sufficiently narrow compared to the full width at half-maximum of the filter. The value of ϕ_A is usually determined so that the value of the Hv component $\tilde{n}^2_{(benzene)}\phi_A I_{Hv(benzene)}$ of the reduced intensity of the light scattered from pure benzene measured at a scattering angle of 90° by the use of the photometer may coincide with the value of the Hv component $R_{Hv(benzene)}$ of the reduced intensity absolutely determined, where $I_{Hv(benzene)}$ is the (total) intensity of the Hv component measured under the same conditions of the apparatus (including the sample cell) as in the case of the measurements on the test solutions but without the narrow band-pass filter. Then ϕ_A may be obtained from

$$\phi_A = R_{Hv(benzene)}/\tilde{n}^2_{(benzene)} I_{Hv(benzene)} \quad (3)$$

$R_{Hv(benzene)}$ is a quantity depending only on the pressure, temperature, and wavelength of the incident light and must therefore be determined without the narrow band-pass filter, so that the intensity $I_{Hv(benzene)}$ (relative to the WS) must also be determined without the narrow band-pass filter.

The value of $R_{Hv(benzene)}$ at 28.0 °C we used is 8.16×10^{-6} cm^{-1}, which had been determined at 25.0 °C in the previous study.[12] We note that $I_{Hv(benzene)}$ and therefore $R_{Hv(benzene)}$ are almost independent of temperature in its range from 25.0 to 28.0 °C, as mentioned previously.[12] The values of the refractive index we used for benzene and CH_3CN at 28.0 °C are 1.518 and 1.345, respectively.

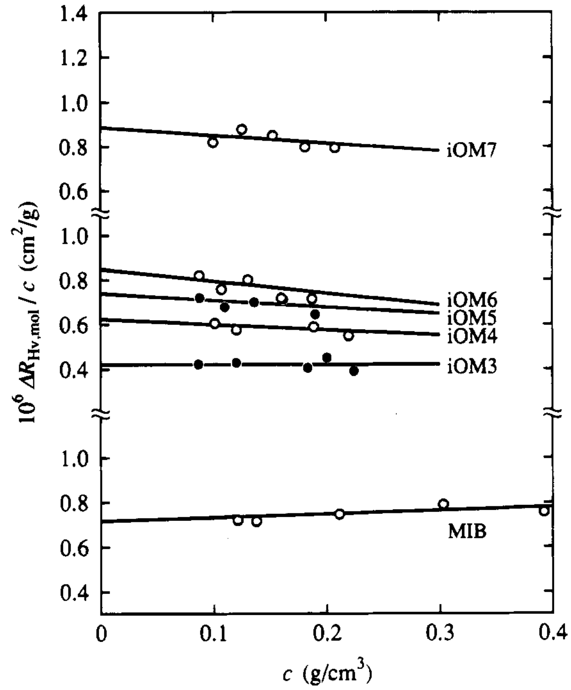

Figure 3. Plots of $\Delta R_{Hv,mol}/c$ against c for i-PMMA samples iOM3 through iOM7 and MIB in CH_3CN at 28.0 °C.

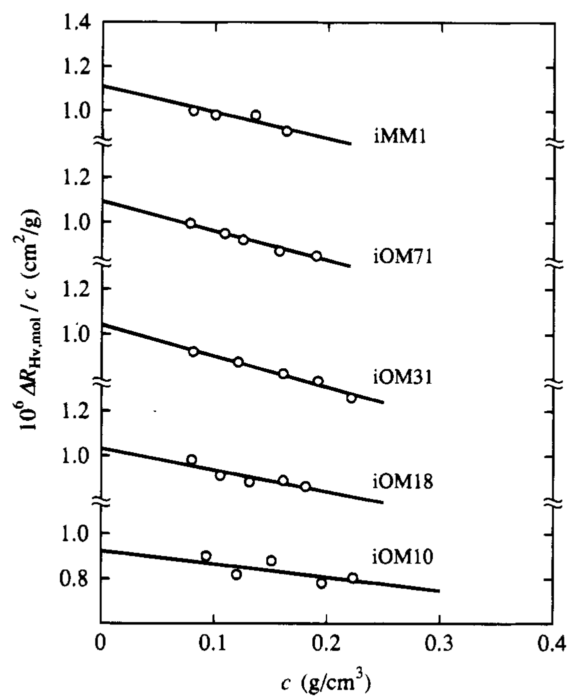

Figure 4. Plots of $\Delta R_{Hv,mol}/c$ against c for i-PMMA samples iOM10 through iMM1 in CH_3CN at 28.0 °C.

Results

Figure 3 shows plots of the ratio of the intrinsic molecular excess depolarized component $\Delta R_{Hv,mol}$ of the reduced intensity to the mass concentration c against c for the samples iOM3 through iOM7 and MIB in CH_3-CN at 28.0 °C (Θ). Figure 4 shows similar plots for the samples iOM10 through iMM1 in CH_3CN at 28.0 °C. The data points for each sample follow a straight line and can be rather easily extrapolated to infinite dilution

Table 2. Values of $\langle\Gamma^2\rangle/x_w$ for Isotactic Oligo- and Poly(methyl methacrylate)s in Acetonitrile at 28.0 °C

sample	$\langle\Gamma^2\rangle/x_w$, Å^6	sample	$\langle\Gamma^2\rangle/x_w$, Å^6
MIB	4.1_1	iOM10	5.5_1
iOM3	2.8_2	iOM18	6.0_0
iOM4	4.0_1	iOM31	5.9_6
iOM5	4.6_4	iOM71	6.1_9
iOM6	5.2_3	iMM1	6.2_8
iOM7	5.3_8		

to obtain $(\Delta R_{Hv,mol}/c)_{c=0}$. The errors in the extrapolation for the samples iOM6 and iOM10 are somewhat larger than those for the others.

If the effect of the internal field is taken into account by the use of the Lorentz–Lorenz equation as in the previous studies,[11,12] the mean-square optical anisotropy $\langle\Gamma^2\rangle$ may be calculated from

$$\langle\Gamma^2\rangle = \frac{15\lambda_0^{\ 4}}{16\pi^4}\frac{M}{N_A}\left(\frac{3}{\tilde{n}^2+2}\right)^2(\Delta R_{Hv,mol}/c)_{c=0} \qquad (4)$$

with the observed value of $\Delta R_{Hv,mol}$ determined above, where λ_0 is the wavelength of the incident light in a vacuum and is equal to 488 nm, M is the solute molecular weight, N_A is Avogadro's number, and $\tilde{n}$ is the refractive index of the solvent. We have already discussed the adoption of the internal field correction of the second power type in eq 4 in the previous study.[12] As mentioned there, this adoption is only a matter of convenience for a comparison of the present results with the previous ones and also with literature data and may be considered to be sufficient for the present main purpose that we analyze the dependence of $\langle\Gamma^2\rangle/x_w$ on x_w on the basis of the HW model.

The values of $\langle\Gamma^2\rangle/x_w$ for all the i-PMMA samples along with that for MIB calculated from eq 4 with the values of $(\Delta R_{Hv,mol}/c)_{c=0}$ determined above are given in Table 2. The value 4.1_1 Å^6 of $\langle\Gamma^2\rangle/x_w$ for MIB is in good agreement with the previous value[12] 4.1_6 Å^6 obtained at 44.0 °C, indicating that the difference between the measurement temperatures in the present and previous[12] studies does not cause any appreciable changes in possible effects of the optically anisotropic solvent CH_3CN.

Figure 5 shows plots of $\langle\Gamma^2\rangle/x_w$ against the logarithm of x_w for i-PMMA in CH_3CN at 28.0 °C (Θ). The solid curve connects smoothly the data points for $x_w \geq 3$, and the dashed line segment connects those for $x_w = 1$ and 3. It is seen that as x_w is increased from unity, $\langle\Gamma^2\rangle/x_w$ (the mean-square optical anisotropy per repeat unit) is first reduced nearly to half at $x_w = 3$, then increases rather steeply to $x_w \simeq 7$, and finally approaches a constant asymptotic value. From Figure 5, this value is estimated to be ca. 6.2 Å^6, which is smaller than the value 7.8 Å^6 for a-PMMA in CH_3CN at 44.0 °C and is about 1 order of magnitude smaller than the value 61 Å^6 for a-PS.[12]

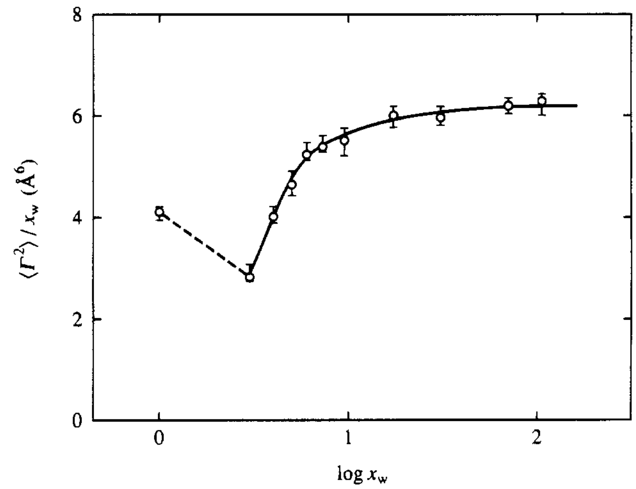

Figure 5. Plots of $\langle\Gamma^2\rangle/x_w$ against log x_w for i-PMMA with $f_r \simeq 0.01$ in CH_3CN at 28.0 °C. The solid curve connects smoothly the data points for $x_w \geq 3$.

Discussion

Comparison with the HW Theory. The conformational behavior of the HW chain[4,5] may be described in terms of the three model parameters: the constant differential geometrical curvature κ_0 and torsion τ_0 of its characteristic helix taken at the minimum zero of its elastic energy and the static stiffness parameter λ^{-1}. For a comparison of the theory with experiment, the shift factor M_L defined as the molecular weight per unit contour length is necessary in order to convert the total contour length L of the HW chain into M by the relation $M = M_L L$. In addition to the above four basic model parameters, the local polarizability tensor $\boldsymbol{\alpha}$ per unit contour length is necessary in the present case of anisotropic scattering.

Now the mean-square optical anisotropy $\langle\Gamma^2\rangle$ of the HW chain of total contour length L (without excluded volume) may be written in the form[11,16]

$$\langle\Gamma^2\rangle = \lambda^{-1}L\sum_{j=0}^{2}C_j(\boldsymbol{\alpha}, \kappa_0/\nu, \tau_0/\nu)\,f_j(\lambda L, \lambda^{-1}\nu) \qquad (5)$$

where ν, C_j, and f_j are given by

$$\nu = (\kappa_0^{\ 2} + \tau_0^{\ 2})^{1/2} \qquad (6)$$

$$C_0(\boldsymbol{\alpha}, x, y) = \frac{1}{2}[2\alpha_{\zeta\zeta} - \alpha_{\xi\xi} - \alpha_{\eta\eta} - 3x^2(\alpha_{\zeta\zeta} - \alpha_{\eta\eta}) + 6xy\alpha_{\eta\zeta}]^2$$

$$C_1(\boldsymbol{\alpha}, x, y) = 6[xy(\alpha_{\eta\eta} - \alpha_{\zeta\zeta}) + (2y^2 - 1)\alpha_{\eta\zeta}]^2 + 6(x\alpha_{\xi\eta} + y\alpha_{\zeta\xi})^2 \qquad (7)$$

$$C_2(\boldsymbol{\alpha}, x, y) = \frac{3}{2}(\alpha_{\xi\xi} - y^2\alpha_{\eta\eta} - x^2\alpha_{\zeta\zeta} + 2xy\alpha_{\eta\zeta})^2 + 6(y\alpha_{\xi\eta} + x\alpha_{\zeta\xi})^2$$

$$f_j(x, y) = (j^2y^2 + 36)^{-2}\{6(j^2y^2 + 36) + (j^2y^2 - 36)x^{-1} + x^{-1}e^{-6x}[(36 - j^2y^2)\cos(jxy) - 12jy\sin(jxy)]\} \qquad (8)$$

with α_{ij} ($i, j = \xi, \eta, \zeta$) being the ij component of the tensor $\boldsymbol{\alpha}$ expressed in a localized Cartesian coordinate system (ξ, η, ζ) affixed to the HW chain. We note that the procedure of the assignment of the localized system to the repeat unit [CH_2–$C^\alpha(CH_3)(COOCH_3)$–CH_2] of the PMMA chain has already been established for both the i- and syndiotactic (s-) PMMA chains in the previous analysis[17] of the rotational isomeric state model[18] data for the angular correlation functions.

For the calculation of the HW theoretical values of $\langle\Gamma^2\rangle$ for i-PMMA from eq 5, we use the values of the basic model parameters previously[1] determined from an analysis of the dependence of $\langle S^2\rangle/x_w$ on x_w, i.e., $\lambda^{-1}\kappa_0 =$

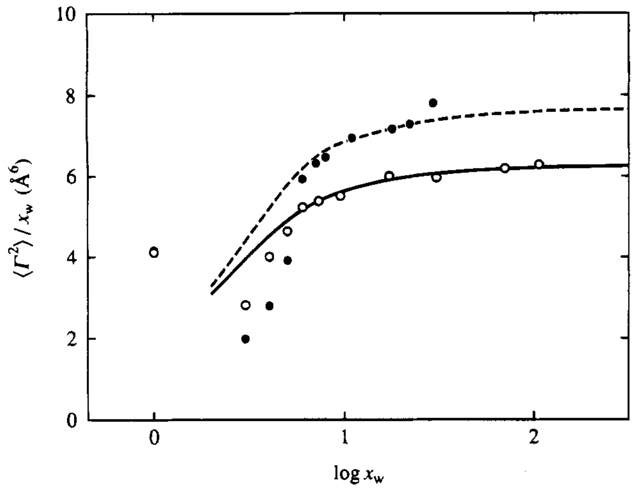

Figure 6. Plots of $\langle\Gamma^2\rangle/x_w$ against log x_w: (○) i-PMMA with $f_r \simeq 0.01$ in CH_3CN at 28.0 °C; (●) a-PMMA with $f_r = 0.79$ in CH_3CN at 44.0 °C.[12] The solid and dashed curves represent the best-fit HW theoretical values for i- and a-PMMAs, respectively.

2.5, $\lambda^{-1}\tau_0 = 1.3$, $\lambda^{-1} = 38.0$ Å, and $M_L = 32.5$ Å^{-1}. As for α, we may calculate it from

$$\alpha = (M_L/M_0)\alpha_0 \tag{9}$$

where α_0 is the polarizability tensor of the repeat unit of the PMMA chain and M_0 is its molecular weight.

In the previous study of a-PMMA,[12] α_0 has already been evaluated to be

$$\alpha_0 = \begin{pmatrix} 0.581 & \pm 0.266 & 0 \\ \pm 0.266 & 0.712 & 0 \\ 0 & 0 & -1.293 \end{pmatrix} (\text{Å}^3) \tag{10}$$

in the localized system. Recall that the components of the traceless α_0 given by eq 10 have been evaluated by the use of the literature values of the bond polarizabilities[10,19,20] for C–C and C–H and of the polarizability tensor for methyl acetate or MIB.[21] The sign of the $\xi\eta$ and $\eta\xi$ components is determined according to the pair of successive bond chiralities defined in the new Flory convention,[22] i.e., plus for *ld* and minus for *dl*. In the case of a-PMMA with large f_r (or s-PMMA) previously[12] considered, the pair of successive bond chiralities of the repeat unit, and therefore the sign of the $\xi\eta$ and $\eta\xi$ components, changes alternately along the chain, so that those components have been put equal to zero on the average. In the present case of the i-PMMA chain, we use the α_0 given by eq 10, where either sign of the $\xi\eta$ and $\eta\xi$ components may be taken, as seen from eqs 7, 9, and 10.

Now the HW theoretical values may be calculated from eq 5 with eqs 6–9 with the above values of the HW model parameters and with α_0 given by eq 10, which must be multiplied by the same factor 0.73 as that previously[12] introduced, as mentioned in the Introduction. Recall that the reduced contour length λL in eq 5 is related to x_w by the equation

$$\log x_w = \log(\lambda L) + \log(\lambda^{-1}M_L/M_0) \tag{11}$$

Figure 6 shows plots of $\langle\Gamma^2\rangle/x_w$ against the logarithm of x_w for i-PMMA in CH_3CN at 28.0 °C. The unfilled circles represent the observed values, and the solid curve represents the HW theoretical values thus calculated. It is seen that the theory may explain quantitatively the behavior of the data points for $x_w \geq 6$. The theoretical values are overestimated for $x_w \leq 5$. This may be regarded as arising from effects of chain ends that have not been taken into account in the HW theory of $\langle\Gamma^2\rangle$.

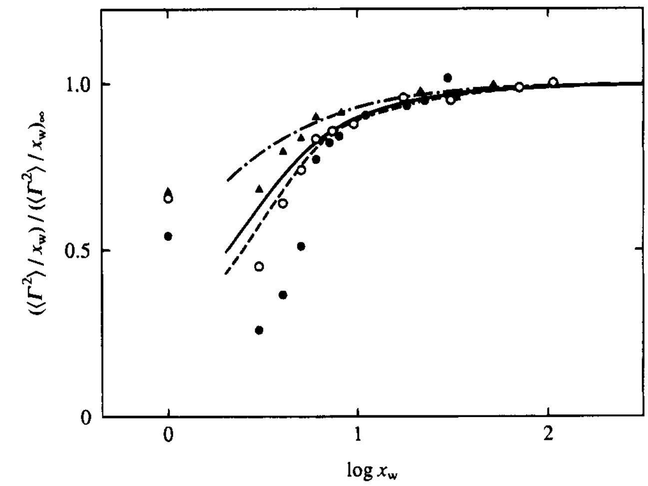

Figure 7. Plots of $(\langle\Gamma^2\rangle/x_w)/(\langle\Gamma^2\rangle/x_w)_\infty$ against log x_w: (○) i-PMMA with $f_r \simeq 0.01$ in CH_3CN at 28.0 °C; (●) a-PMMA with $f_r = 0.79$ in CH_3CN at 44.0 °C;[12] (▲) a-PS with $f_r = 0.59$ in cyclohexane at 34.5 °C.[11] The solid, dashed, and chain curves represent the best-fit HW theoretical values for i-PMMA, a-PMMA, and a-PS, respectively.

Comparison with the a-PMMA and a-PS Chains. In Figure 6 are also plotted the previous data for a-PMMA with $f_r = 0.79$ in CH_3CN at 44.0 °C (Θ) (filled circles) along with the corresponding HW theoretical values (dashed curve). As in the case of i-PMMA, the latter values for a-PMMA have been calculated from eq 5 with the values of the HW model parameters determined from $\langle S^2\rangle$.[6] It is seen that the asymptotic value $(\langle\Gamma^2\rangle/x_w)_\infty$ in the limit $x_w \to \infty$ for i-PMMA is appreciably smaller than that for a-PMMA, as already mentioned in the Results, and that this difference, which arises from that in f_r, may be explained satisfactorily by the HW theory. It is interesting to note that, in contrast to this dependence of $(\langle\Gamma^2\rangle/x_w)_\infty$ on f_r, the asymptotic value $(\langle S^2\rangle/x_w)_\infty$ for i-PMMA is appreciably larger than that for a-PMMA[1] and therefore that the values of $[\eta]$ and the hydrodynamic radius R_H (determined from D) in the range of large M_w for the former are larger than the respective values for the latter.[3] The above difference in the f_r dependence between $\langle\Gamma^2\rangle$ and the three quantities $\langle S^2\rangle$, $[\eta]$, and R_H may be understood, since the last three reflect directly the average dimension of polymer chains but this is not necessarily the case with $\langle\Gamma^2\rangle$. As x_w is decreased, $\langle\Gamma^2\rangle/x_w$ decreases more steeply for a-PMMA than for i-PMMA, becoming smaller for the former than for the latter for $x_w \leq 5$. This difference in the x_w dependence between the i- and a-PMMAs may be considered to reflect, to some extent, the difference in the chain conformation between them. For very small x_w, however, it may probably be mainly due to effects of chain ends, since those of the i-PMMA samples used are a hydrogen atom and a *tert*-butyl group, and those of the a-PMMA samples used are both hydrogen atoms.

Finally, we compare the present results for the two PMMAs with the previous ones for a-PS.[11] As mentioned in the Results, the value of $(\langle\Gamma^2\rangle/x_w)_\infty$ for a-PS is about 1 order of magnitude larger than those for the i- and a-PMMAs, so that attention is given only to the relative x_w dependence of $\langle\Gamma^2\rangle/x_w$. Figure 7 shows plots of $(\langle\Gamma^2\rangle/x_w)/(\langle\Gamma^2\rangle/x_w)_\infty$ against the logarithm of x_w. The unfilled and filled circles represent the values for the i- and a-PMMAs corresponding to those in Figure 6, and the filled triangles represent the values for a-PS in cyclohexane at 34.5 °C (Θ).[11] Except for the data points corresponding to the monomers, i.e., MIB for the two PMMAs and cumene for a-PS, the ratio $(\langle\Gamma^2\rangle/x_w)/(\langle\Gamma^2\rangle/x_w)_\infty$ increases monotonically with increasing x_w and approaches unity in each case. The steepness of the increase in the range of small x_w is larger for a-PMMA and smaller for a-PS than for i-PMMA. Clearly, this difference arises from that in the local chain conformation between them, and it is seen that the HW theory may give a good explanation of it.

Conclusion

For i-PMMA with $f_r \simeq 0.01$ in acetonitrile at 28.0 °C (Θ), the mean-square optical anisotropy $\langle\Gamma^2\rangle$ has been determined rather unambiguously. It has then been shown that the results thus obtained for $x_w \geq 6$ may be quantitatively reproduced by the HW theoretical values calculated with the model parameters previously[1] determined from $\langle S^2\rangle$ and with the local polarizability tensor α_0 of the repeat unit of the i-PMMA chain evaluated with the same bond polarizabilities as in the previous case of a-PMMA[12] (along with the same factor 0.73). Thus it is concluded that the HW model may give a consistent explanation of the f_r dependence of a variety of dilute solution properties such as $\langle S^2\rangle$, $P(k)$, $\langle\Gamma^2\rangle$, $[\eta]$, and D. All the differences in these properties between the i- and a-PMMAs arise from the fact that the former chain is of weaker helical nature than the latter, which retains rather large and clearly distinguishable helical portions in dilute solution.[1] The disagreement between theory and experiment for $\langle\Gamma^2\rangle$ for i-PMMA in the range of very small x_w (≤ 5) may probably be due to effects of chain ends as in the cases of a-PMMA[12] and a-PS.[11]

References and Notes

(1) Kamijo, M.; Sawatari, N.; Konishi, T.; Yoshizaki, T.; Yamakawa, H. *Macromolecules* **1994**, *27*, 5697.
(2) Horita, K.; Yoshizaki, T.; Hayashi, H.; Yamakawa, H. *Macromolecules* **1994**, *27*, 6492.
(3) Sawatari, N.; Konishi, T.; Yoshizaki, T.; Yamakawa, H. *Macromolecules* **1995**, *28*, 1089.
(4) Yamakawa, H. *Annu. Rev. Phys. Chem.* **1984**, *35*, 23.
(5) Yamakawa, H. In *Molecular Conformation and Dynamics of Macromolecules in Condensed Systems*; Nagasawa, M., Ed.; Elsevier: Amsterdam, 1988; p 21.
(6) Tamai, Y.; Konishi, T.; Einaga, Y.; Fujii, M.; Yamakawa, H. *Macromolecules* **1990**, *23*, 4067.
(7) Fujii, Y.; Tamai, Y.; Konishi, T.; Yamakawa, H. *Macromolecules* **1991**, *24*, 1608.
(8) Yoshizaki, T.; Hayashi, H.; Yamakawa, H. *Macromolecules* **1993**, *26*, 4037.
(9) Yamakawa, H.; Shimada, J.; Fujii, M. *J. Chem. Phys.* **1978**, *68*, 2140.
(10) Patterson, G. D.; Flory, P. J. *J. Chem. Soc., Faraday Trans. 2* **1972**, *68*, 1098, and succeeding papers.
(11) Konishi, T.; Yoshizaki, T.; Shimada, J.; Yamakawa, H. *Macromolecules* **1989**, *22*, 1921.
(12) Takaeda, Y.; Yoshizaki, T.; Yamakawa, H. *Macromolecules* **1993**, *26*, 3742.
(13) Takaeda, Y.; Yoshizaki, T.; Yamakawa, H. *Macromolecules* **1995**, *28*, 682.
(14) Ute, K.; Asada, T.; Miyatake, N.; Hatada, K. *Makromol. Chem., Macromol. Symp.* **1993**, *67*, 147.
(15) Hermans, J. J.; Levinson, S. *J. Opt. Soc. Am.* **1951**, *41*, 460.
(16) Yamakawa, H.; Fujii, M.; Shimada, J. *J. Chem. Phys.* **1979**, *71*, 1611.
(17) Yamakawa, H.; Shimada, J. *J. Chem. Phys.* **1979**, *70*, 609.
(18) Flory, P. J. *Statistical Mechanics of Chain Molecules*; Interscience: New York, 1969.
(19) Patterson, G. D.; Flory, P. J. *J. Chem. Soc., Faraday Trans. 2* **1972**, *68*, 1111.
(20) Suter, U. W.; Flory, P. J. *J. Chem. Soc., Faraday Trans. 2* **1977**, *73*, 1521.
(21) Flory, P. J.; Saiz, E.; Erman, B.; Irvine, P. A.; Hummel, J. P. *J. Phys. Chem.* **1981**, *85*, 3215.
(22) Flory, P. J.; Sundararajan, P. R.; DeBolt, L. C. *J. Am. Chem. Soc.* **1974**, *96*, 5015.

MA946228M